



# Production of hydrogen- and methane-rich gas by stepped pyrolysis of biomass and its utilization in IC engines

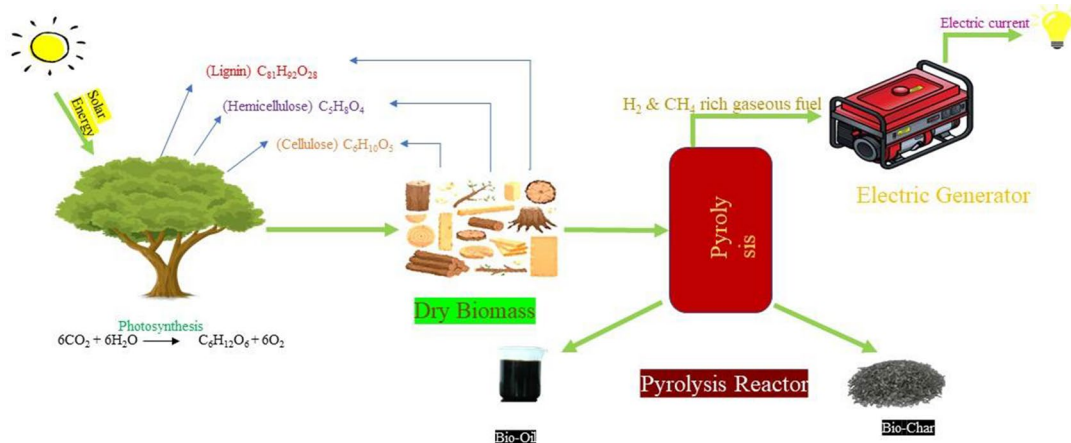
Brijesh Kumar Prajapati<sup>1</sup> · Amrit Anand<sup>1</sup> · Shalini Gautam<sup>1</sup> · Preetam Singh<sup>2</sup>

Received: 27 April 2021 / Accepted: 28 November 2021 / Published online: 18 January 2022  
© The Author(s), under exclusive licence to Springer-Verlag GmbH Germany, part of Springer Nature 2021

## Abstract

Automobile industries primarily use petroleum-based fuels like petrol and diesel, creating environmental hazards, a high carbon footprint, and severe health issues. The world focuses on compressed natural gas (CNG)-based energy solutions and developing CNG infrastructures to minimize environmental concerns from fossil fuel. The current focus to introduce a fraction of hydrogen with CNG in the existing fuel system is initiated here. Therefore, biomass utilization is taken into account to produce high hydrogen-containing fuel to cut down the carbon footprint and environmental issues. Biomass residues such as sun hemp, pigeon pea, mustard stem, wheat straw, dhaincha, and vantulasi were slowly pyrolyzed in a stepped manner to produce a hydrogen-rich clean fuel. The yield of product gas (hydrogen-rich CNG; HCNG) obtained by the pyrolysis process (21–29%) contains a volumetric composition of 40–55% hydrogen and 10–25% methane balanced with oxides of carbon depending on different biomass feedstocks. This study also focused on utilizing obtained HCNG in IC engine (2KVA Honda Genset) in terms of its running duration and efficiency. The maximum running time observed in sun hemp is 30 min, followed by the mustard stem is 28 min, the lowest in vantulasi is 16 min. However, the highest process efficiency is 87% for dhaincha which is 3.6 times more effective, and the lowest is 74% for Sun hemp, which is 3 times more effective than petrol in Genset for power production. A correlation is developed between ultimate analysis and product gas composition for running time estimation.

## Graphical abstract



**Keywords** Bio-HCNG · Ultimate analysis · Pyrolysis · Gas chromatography · IC engines

✉ Shalini Gautam  
shalinigautam@iitism.ac.in

Extended author information available on the last page of the article

## Introduction

Energy is the lifeblood of human society; imagining the world without a continuous energy supply is impossible; currently, fossil fuels fulfill a significant portion of energy demand. However, the constant supply of fossil fuels is becoming a challenge in recent years resulting in a continuous price rise (Edwards et al. 2007; Pawar et al. 2013). Further, the exhausts resulting from the combustion of these fossil fuels are very dangerous for human beings and the environment, leaving a huge carbon footprint behind (Reşitoğlu et al. 2015). The interrelated problems of energy and the environment are one of the biggest challenges the world is facing today. Energy sustainability and the decreasing carbon footprint are the biggest challenge that must be attained and rectified in an accelerated way. The thermochemical conversion route is an excellent solution to use biomass energy in technical applications (Chen et al. 2003). The world is moving toward CNG and HCNG (a mixture of hydrogen and CNG) to minimize the environmental pollution caused due to exhaust gases from IC engines and industries (Lang et al. 2011; Jiang et al. 2012; Abuadala and Dincer 2012).

Hydrogen has many positive characteristics while using in internal combustion engines, such as better flammability and improved performance of engines that make HCNG more advantageous over CNG (Moreno et al. 2012). The hydrogen fuel system produces water vapor, which is eco-friendly. So it can be adopted as a future fuel because of its different characteristics like rapid burning speed, no emissions of greenhouse gases, higher energy density, low minimum ignition energy, and a very high octane number (Mu et al. 2006; Balat and Kirtay 2010; Luque et al. 2011; Momin et al. 2016).

The immediate replacement of fossil fuel systems with a pure hydrogen system is a gigantic task and must be attained stepwise in the future. One of the alternatives is to replace a proportion of hydrogen with methane, so that smooth transfer from petroleum-based technology to hydrogen-based technology can be done (Nanthagopal et al. 2011). There are many conventional and established ways to obtain  $H_2$  and  $CH_4$  mixture, but they can only be environmentally friendly if extracted from renewable energy sources like biomass other than fossil fuels. Hydrogen can be obtained from syngas, alkane steam reforming, electrosynthesis (Sadhukhan et al. 2016), and dark fermentation processes whose main gaseous component is hydrogen. However, methane can be obtained from the anaerobic digestion process (Liu et al. 2018).

Agricultural and forestry wastes are carbon neutral potential sources of renewable energy. The estimation of bio-waste produced each year is about 120 billion tons,

generating five times the world's current energy consumption. Only 1% of the total energy capacity uses as energy, which can supply 14% of total energy consumption in the world. However, most biomass waste goes under bacterial decomposition or combustion, which results in GHG emissions into the atmosphere (Mengjie and Suzhen 1994).

A two-stage anaerobic digestion process was reported recently to get Bio-HCNG in different proportions (Luo et al. 2011; (David et al. 2019). Sometimes hydrogen and methane are produced separately, and to get HCNG different appropriate proportion of hydrogen and methane is mixed. The main routes to produce hydrogen from agricultural and forestry residues are namely thermochemical and biochemical processes. Thermochemical routes can adopt for continuous and rapid utilization of biomass. Thermochemical routes are combustion, gasification (Chang et al. 2011), pyrolysis (Xu et al. 2010). The main route of getting methane from bio-wastes is anaerobic digestion (Gunaseelan 1997).

Gasification is a process where hydrocarbons undergo partial combustion, and the main product is synthesis gas. Slow pyrolysis is a process in which bio-organic materials undergo thermal degradation in a completely oxygen-free atmosphere. At the end of biomass pyrolysis, one can get solid (biochar), liquid (bio-oil), and biogas [a mixture of  $H_2$ ,  $CO$ ,  $CH_4$ ,  $CO_2$ , and lower hydrocarbon of ( $C_1-C_3$ )] (Karagöz 2009). Biomass structures also define the proportion of different pyrolytic products and the composition of the gaseous product. The heating rate significantly affects the pyrolytic product composition (Debdoubi et al. 2006). As lignin is responsible for high  $H_2$  and  $CH_4$  formation, hemicellulose is responsible for increased  $CO_2$  emissions, and cellulose is responsible for high  $CO$  production (Hlavsová et al. 2014). The hydrogen ( $H_2$ ) content is dependent on the temperature of pyrolysis and increases as the latter increases (Li et al. 2004; Domínguez et al. 2007; Dufour et al. 2009; Neves et al. 2011). The conversion of raw biomass to the gaseous product during the pyrolysis process is high (Zhao et al. 2001). The pyrolysis process route uses to produce liquid fuel from biomass, not a gaseous fuel. This study mainly focuses on the production of gaseous fuel rather than liquid fuel.

Previous studies have been the approach for syngas production through gasification route and hydrogen enrichment through steam reforming, methane reforming, and water gas shift reaction (Chimpae et al 2019). This study explains the biomass utilization potential for hydrogen production from the pyrolysis route and utilization in the IC engine. For analyzing the running time performance of 2KVA Honda petrol Genset with the product gas composition and ultimate analysis, a correlation is developed between  $H_2$ ,  $CH_4$ ,  $\Delta H$  (change in hydrogen wt% during the process), and  $D$  (Duration for which Genset will run in minutes).

The pyrolyzed gas has several advantages, such as higher heating value, higher hydrogen content than conventional syngas. Therefore, it can be applied well to the downstream gas turbine/combustion engines to generate power or used for other civil purposes (Chen et al. 2003).

The present work describes biomass composition, conversion process, the yield of gaseous products w.r.t. temperature, and performance of the gaseous product in IC engine (Spark Ignition only). The gaseous product was obtained during the stepped pyrolysis of different agricultural residues in a fixed bed reactor. However, HCNG can also utilize in the CI (Compression Ignition) engine (Zareei et al. 2020). This paper explores the method to produce high-yield hydrogen and methane or HCNG in a single process from various agricultural wastes.

## Materials and methods

### Sample collection and preparation

Biomass is carbon-neutral fuel and is abundantly available in India. The total production of biomass is around 750MT, out of which the surplus availability is 230 MT (Mnre report). In this study, the agricultural waste like pigeon pea (PP), sun hemp (SH), mustard stem (MS), wheat straw (WS), dhaincha (DH) (*sesbania bispinosa*) and forestry waste like vantulasi (VT) (*Ocimum Gratissimum*) were used as biomass feed. Table 1 explains the selective biomass availability, cost, and potential in India.

Vantulasi grows in the Himalayas and Vindhya region and the plains of India, where it grows as a naturalized plant. Vantulasi is also cultivated and grows wild through Asia and Africa. Dhaicha cultivates before rice cultivation throughout India (Green-talk). These samples were collected from the village area of Varanasi and the forestry area of the Mirzapur District of Uttar Pradesh, India. The biomass samples were first dried in a normal atmosphere for 5–10 days and then chopped and milled in the size range of <2 inches. Then the sample was oven-dried at 105 °C for 24 h. The biomass

samples were prepared in the size range of – 18# + 72# and utilized for different analyses.

### Reactor setup and testing: reactor design/setup and attached testing facility layout are shown in Fig. 1

The biomass conversion was performed under anaerobic conditions in a pyrolysis reactor. The reactor setup consists of a quartz reactor, and a tripod sample holder is there which holds the sample inside the heating zone, and a furnace with a PID controller. A toggle valve at the bottom of the reactor facilitates the nitrogen flow inside the reactor to maintain an inert environment. Setup is also provided with an electric resistance furnace for indirect heating the charge, and a pressure regulator is there to show and control the pressure inside the reactor. A condenser is also attached at the reactor outlet to separate condensable (Bio-oil + water) from non-condensable gas. Non-condensable gas was collected in a gas collector, and intermediate gas sampling was carried out to get the product gas composition at different temperatures. Product gases were analyzed by gas chromatography (GC) (MM TECH, M 2012) equipped with a molecular sieve pack column and thermal conductivity detector (TCD). The analysis was carried out using (N 2000) software attached with the instrument.

### Experimental procedure

Biomass decomposes into valuable cleaner fuel under anaerobic conditions at elevated temperatures in a vertical reactor in the pyrolysis route. In this process, the biomass samples of <2 inches size were fed into the reactor. N<sub>2</sub> gas was purged (1lpm) to maintain an inert environment inside the reactor. The reactor is heated at a rate of 15 °C/min to the temperature of 150 °C after maintaining the inert atmosphere. Once the pressure inside the reactor reached up to 1.1 bar at 150 °C, the vapor drains out.

Further nitrogen is purged into the reactor to remove the reactant gases to maintain the inert atmosphere, and after that, the valve was closed. The reactor temperature rises to

**Table 1** Biomass availability in India (IISCR report; Paul and Rahaman 2015)

Sample Name	Biomass Generation (KT/year)	Surplus Availability (KT/year)	MWe	Feed cost (Rs/kg) (Raw material + Preparation + Transportation)
SH	14.1	1.41	0.18	2.5
PP	5120.2	822	101.7	2.0
MS	6998.3	3173.9	412.6	2.0
WS	93,361.7	16,176.3	2102.9	3.0
DH	NA	NA	NA	1.5
VT	NA	NA	NA	1.5

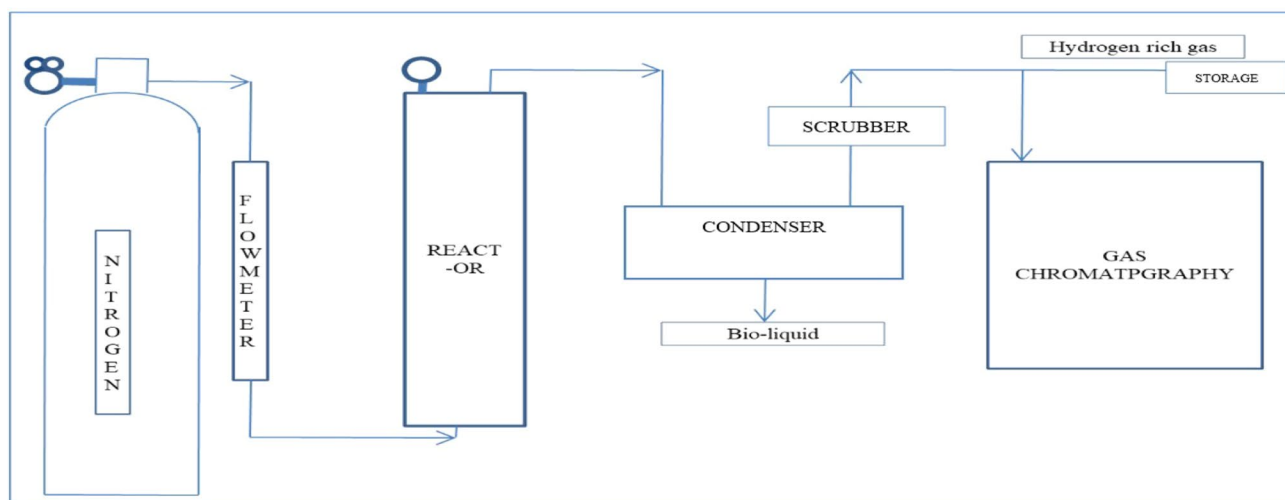


Fig. 1 Flowchart of the pyrolysis process

800 °C at a heating rate of 25 °C/mine. At 400 °C, the valve was opened. The product gas was collected and analyzed after passing through the condenser and scrubber. Similarly, at 600 °C, 700 °C, 800 °C and also after 5 min at 800 °C, the product gas was collected and analyzed.

## Results and discussion

### Proximate analysis of biomass samples

Proximate analysis of the biomass samples was carried out as per ASTM standards E871-82, E1755-01, and E872-82 (Suman and Gautam 2017). Biomass char was also prepared following ASTM standards D1762-84 (Suman and Gautam 2017); the result of the proximate analysis is given in Table 2.

Table 2 contains a dry basis proximate analysis of different biomass and their respective chars. All biomass samples have high volatile matters; SH, PP, VT, and DH have about 78% volatile matter. In char, we can see the

extent of the evolution of volatile matter @ 800 °C (VM) into valuable gases. The highest evolution of VM is taken place in SH (nearly 68%), followed by WS (almost 62%) and DH (nearly 66%). High VM is desirable in the present study. After stepped pyrolysis (a series of devolatilization reactions) that progressively leave behind an increasingly condensed carbonaceous matrix, which is nothing but fixed carbon and ash, higher fixed carbon in biochar indicates higher energy value for the respective char (Ronsse et al. 2013). DH, SH, and PP chars are having about 83–79% of fixed carbon. Lower the ash content better will be the fuel quality and, at the same time, lesser problematic in operations. The mustard stem char contains 18.5% of ash, and the WS char has 27.25% ash content, which is higher among all the above samples.

Higher the fixed carbon in biomass, higher the biochar yield, while higher volatile matter and ash content in biomass results in lesser biochar yield (Nunes et al. 2017). Therefore, higher volatile content leads to higher gas production than the solid phase (Nunes et al. 2018).

**Table 2** Proximate analysis and GCV of biomass and char (\*db)

Sample name	Volatile matter wt%		Fixed carbon wt%		Ash content wt%		Gross calorific value (cal./gm)	
	Raw	Char	Raw	Char	Raw	Char	Raw	Char
SH	78.46	9.57	10.4	80.88	11.13	9.54	4143	6431
PP	71.65	7.8	15.73	79.51	12.61	12.68	4454	6264
MS	78.37	16.96	12.60	64.50	9.02	18.52	4264	5994
WS	70.48	8.12	15.92	64.62	13.58	27.25	4081	5456
VT	77.69	15.64	17.5	72.13	4.81	12.22	3941	6081
DH	77.61	11.05	17.47	83.26	4.9	5.67	4184	6899

\*Dry basis

## Elemental analysis

The elemental (C, H, N, S, and O) analysis of these biomass materials was analyzed by Vario elemental analyzer (IIT (ISM) Dhanbad) using standard ASTM E777, 778, and 775 (Hernandez-Mena et al. 2014). The C, H, N, S, and O were calculated on the ash and moisture-free basis given in Table 3.

### Carbon and hydrogen content

From Table 3, it is observed that the carbon content in raw biomass samples lies between (47–56.13%) and char (89.31–95.42%). During solid fuel combustion (coal, biomass, etc.), the carbon comes out as CO<sub>2</sub> and hydrocarbons. CO<sub>2</sub> can produce from the organic compounds, but carbonate (e.g., calcite–CaCO<sub>3</sub>) minerals are present in the sample, then it can be liberated from there also (Mazzotti et al. 2005). Total carbon measurement may include both fixed carbon and volatile carbon fraction. After pyrolysis processing, the carbon percentage increases due to removing aromatic hydrocarbons, short- and long-chain hydrocarbons, and sulfur (VM) are well represented in Table 3.

The hydrogen content in studied raw samples lies in the range of (6.93–7.77%) and char (1.62–2.49%). Hydrogen is the most critical element in this investigation; this will be responsible for hydrogen production and methane production. Higher the hydrogen content, the better the fuel is. Hydrogen is mainly generated from the condensation of aromatics or alkyl aromatization reaction during pyrolysis at a temperature beyond 400 °C (Liu et al. 2020). Thus, these plants can act as a good source of hydrogen. The difference of hydrogen in raw and char after pyrolysis shows the extent of hydrogen evolution during the process, mainly in the form of hydrogen and methane, which is highest in SH and PP. Thus, the high hydrogen-rich fuel can be produced using SH and PP as bio-waste. The C & H content of the sample plays a vital role in the combustibility of any biomass (Loison et al. 1989).

### Nitrogen and sulfur content

From Table 3, it can be observed that nitrogen content in raw biomass samples lies in the range of (0.68–3.19%), and their char lies in the range of (0.70–1.15%). The nitrogen content in SH and PP is a little high which is because they are nitrogenous crops. The amount of sulfur present in raw samples of SH, PP, MS, WS, VT, and DH lies in the range of (0.15–0.48%) and their char in the range of (0.09–0.50%). High sulfur-containing fuel is not suitable for internal combustion engines as well for power production.

The low S- & N-containing biomass consider as a good fuel because there will be a low formation of sulfur and nitrogen oxides during the thermochemical conversion process (Enweremadu and Ojediran 2004). That is an indication that the biomass samples used in this study will not pollute the atmosphere. The sulfur-containing fuel affects adversely on the metal quality due to its corrosive nature toward metal, because of this, sulfur-containing fuels are not fit for IC engines (Loison et al. 1989). Therefore, the biomass used in this work can reduce the corrosion severity impact on the downstream equipment use and thus lower maintenance costs.

### Oxygen content

From Table 3, the amount of oxygen present in raw samples is in (32.48–44.60%) and their char in the range of (1.84–7.19%). Oxygen content is high in WS, VT, and DH, whereas SH and PP have a relatively lower percentage. The thermal decomposition of the oxygen functionality is responsible for the formation of carbon dioxide and carbon monoxide, which is present in the molecular structure of biomass (Nunes et al. 2018). Thus, the oxygen content and conversion should be less for better applicability as a suitable fuel source. In the case of SH and PP having lesser oxygen conversion took place, thus making them a better alternative as bio-waste to produce high hydrogen-containing fuel.

**Table 3** Elemental analysis (wt%, dry basis)

S. no.	Sample name	C (%)		H (%)		N (%)		S (%)		O (%)	
		Raw	Char	Raw	Char	Raw	Char	Raw	Char	Raw	Char
1	SH	53.40	93.48	7.59	1.84	2.62	0.86	0.48	0.17	35.91	3.65
2	PP	56.13	95.42	7.77	1.62	3.19	1.03	0.43	0.09	32.48	1.84
3	MS	52.93	90.24	7.56	2.47	1.00	1.04	0.20	0.35	38.31	5.90
4	WS	47.01	92.44	6.93	2.11	1.13	1.15	0.31	0.50	44.60	3.80
5	VT	48.24	93.15	6.93	2.24	0.68	0.70	0.15	0.17	44.00	3.56
6	DH	50.99	89.31	7.10	2.49	1.07	0.83	0.23	0.17	40.61	7.19

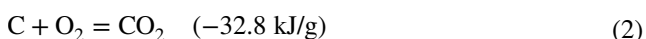
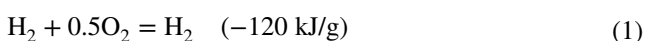
## Calorific values

The combustion of a substance gives energy in the form of heat, which can use for different purposes (the blast furnace, power production, small furnaces, etc.). Volatile matter and fixed carbon are responsible for high calorific values in biomass samples. ASTM D4809-00 standard test method was followed to calculate the calorific value by bomb calorimeter (Make: LECO; Model: AC 350) (Suman et al. 2017).

The calorific value of raw samples lies in the range of 3941–4454 kcal/kg and their char in the range of 5456–6899 kcal/kg, which is shown in Table 2.

Heat of the reaction mainly for hydrogen and carbon is as below-

Heat of reaction:



The above reaction equations indicate that hydrogen contributes more toward calorific value than carbon. So high hydrogen is desirable in a fuel. Raw PP has the highest hydrogen content, nearly 8%, that eventually visualized in its overall highest calorific value. On the other hand, the

calorific values of chars are the result of carbon combustion. The higher the carbon content, the higher will be the calorific value of char. DH char has a high calorific value of about 6900 kcal/kg; this results from a high fixed carbon present in DH.

## Thermogravimetric analysis

The ASTM E1131-03 standard method was used for TGA, using a computerized NETZSCH SAT 449F3 TG analyzer [IIT (ISM) Dhanbad]. The temperature program used for the TGA shown in Fig. 2 starts at room temperature to 105 °C and is further allowed to go up to 800 °C with an increment rate of 25 °C/min in a nitrogenous environment.

The main components of all biomass are lignin, hemicelluloses, cellulose, and extractives. Their concentrations vary in different biomass samples depending on their growth conditions and from species to species. These components decompose during pyrolysis and produce condensable (bio-oil and tar), non-condensable (gases), and solid (char) parts.

From Table 4, the whole TGA is divided into five zones that interpret each component's decomposition as below.

Zone I: < 100 °C mainly moisture evolution takes place in this zone.

**Fig. 2** TGA of MS, SH, WS, DH, PP, and VT Samples

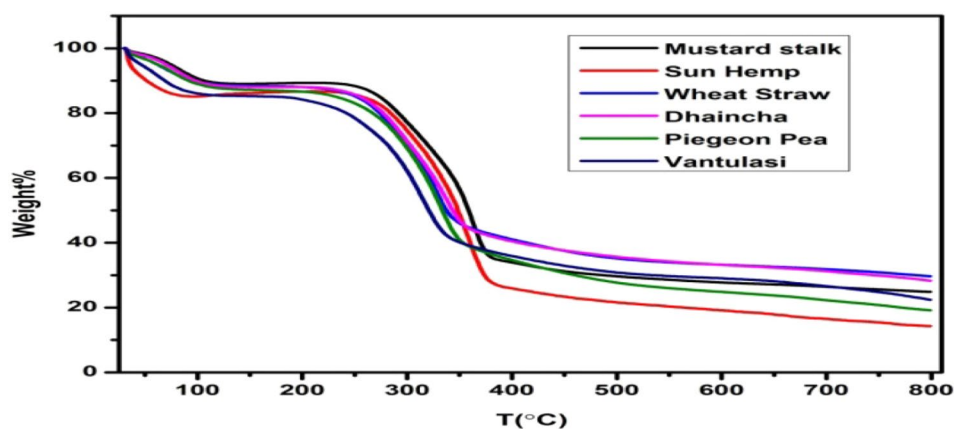


**Table 4** Volatiles released (wt%) during biomass pyrolysis in TGA

Sample name	Moisture zone-I < 100	Volatiles released (%)				
		Temperature range (°C)				
		Zone-II 100–300	Zone-III 300–400	Zone-IV 400–600	Zone-V > 600	Total
SH	15	9	51	5	3	83
PP	12	19	27	11	7	76
MS	10	13	42	9	3	77
WS	11	11	30	10	5	67
DH	10.5	10.5	33	10	9	73
VT	15	26	20	8	6	75

**Table 5** Volumetric composition of produced gas during the slow pyrolysis process of sun hemp

Temperature	Volume %			
	H <sub>2</sub>	CH <sub>4</sub>	CO	CO <sub>2</sub>
600 °C	7.89	35.05	33.23	23.83
700 °C	58.8	24.6	9.8	6.8
800 °C	81.34	12.07	6.35	0.24
<sup>R5</sup> 800 °C	71.41	12.21	7.08	9.30
*Overall	57.22	20.09	10.26	12.43

\*Overall sampling indicates the sample is taken from the gas storage balloon at the end of the process at room temperature

<sup>R5</sup>Samples were collected at 800 °C after 5 min of residence time

**Table 6** Volumetric composition of produced gas during slow pyrolysis process of pigeon pea

Temperature	Volume %			
	H <sub>2</sub>	CH <sub>4</sub>	CO	CO <sub>2</sub>
600 °C	12.8	54.2	16.8	16.2
700 °C	50.8	32.2	11.4	5.6
800 °C	47.08	30.5	10.3	12.12
<sup>R5</sup> 800 °C	52.49	31.3	7.14	9.07
*Overall	52.45	19.82	11.88	15.85

Zone II: 100–300 °C extractive starts decomposing.

Zone III: 300–400 °C predominantly hemicellulose decomposition.

Zone IV: 400–600 °C mainly cellulose and lignin decomposition.

Zone V: > 600 °C mainly lignin decomposition (Raveendran et al. 1996).

Oxygen concentration is higher in the case of hemicelluloses and cellulose as compare to lignin. The above table shows that hemicelluloses and cellulose decomposed at lower temperatures and lignin decomposed at higher temperatures.

### Gas chromatographic analysis

The produced gas was analyzed through gas chromatography (GC); the results of GC for each of the selected biomass samples are shown below (Tables 5, 6, 7, 8, 9, and 10).

Table 5 shows that in sun hemp, hydrogen starts coming out about 600 °C, the evolution of carbon monoxide and carbon dioxide is higher at lower temperatures. Hydrogen content increases as the temperature increases; on the other hand, carbon monoxide and carbon dioxide decrease. Methane is higher at starting, and it started decreasing at 800 °C. The total product gas composition contains nearly

**Table 7** Volumetric composition of produced gas during slow pyrolysis process of mustard stem

Temperature	Volume %			
	H <sub>2</sub>	CH <sub>4</sub>	CO	CO <sub>2</sub>
600 °C	23.6	5.40	35.90	35.10
700 °C	32.05	23.39	23.33	21.23
800 °C	51.30	23.03	12.62	13.05
<sup>R5</sup> 800 °C	55.08	30.02	8.88	6.02
*Overall	52.53	25.65	4.43	17.39

**Table 8** Volumetric Composition of produced gas during slow pyrolysis process of wheat straw

Temperature	Volume %			
	H <sub>2</sub>	CH <sub>4</sub>	CO	CO <sub>2</sub>
600 °C	27.9	43.6	12.8	15.7
700 °C	67.03	16.5	2.49	13.98
800 °C	77.91	13.3	2.16	6.63
<sup>R5</sup> 800 °C	76.3	18.5	1.8	3.40
*Overall	50.29	19.9	9.98	19.83

**Table 9** Volumetric composition of produced gas during slow pyrolysis process of dhaincha

Temperature	Volume %			
	H <sub>2</sub>	CH <sub>4</sub>	CO	CO <sub>2</sub>
600 °C	29.39	29.27	12.47	28.87
700 °C	53.57	27.07	2.95	16.41
800 °C	60.08	25.59	3.85	10.48
<sup>R5</sup> 800 °C	67.2	19.5	4.15	9.15
*Overall	49.95	20.56	9.1	20.39

**Table 10** Volumetric composition of produced gas during slow pyrolysis process of vantulasi

Temperature	Volume %			
	H <sub>2</sub>	CH <sub>4</sub>	CO	CO <sub>2</sub>
600 °C	34.60	8.10	1.33	55.97
700 °C	52.80	17.50	9.20	20.50
800 °C	58.60	19.70	9.58	12.12
<sup>R5</sup> 800 °C	60.34	22.83	3.98	12.85
*Overall	38.12	8.46	1.62	51.8

57% hydrogen, 20% methane, 10.26% carbon monoxide, and 12.43% carbon dioxide.

As evident from Table 6, at 600 °C, hydrogen is 12.8%, methane is 54.2%, carbon monoxide 16.8%, and CO<sub>2</sub> is 16.2%. At 700 °C, hydrogen increases, and CH<sub>4</sub> decreases

but not much; on the other hand, the concentration of CO and CO<sub>2</sub> decreases significantly. Gas composition evolving at further temperatures like at 800 °C and 5 min after reaching 800 °C is almost the same as previously. The overall composition obtained from the product gas of pigeon pea is close to 52.45% H<sub>2</sub>, 19.82% CH<sub>4</sub>, 11.88% CO, and approximately 16% CO<sub>2</sub>. H<sub>2</sub> composition increases from top to bottom w.r.t the increase in temperature; this may be because of the decomposition of lignin at higher temperatures which restricts the disintegration of bonds at lower temperatures.

Table 7 shows that the evolution of H<sub>2</sub> is significant at 600 °C; its concentration is about 23.6%, methane concentration is significantly less, about 5%, and CO, CO<sub>2</sub> is high in concentration. At higher temperatures concentration of H<sub>2</sub> increases, and CH<sub>4</sub> also increases but CO and CO<sub>2</sub> decrease. The final composition of H<sub>2</sub> is about 52%, CH<sub>4</sub> nearly 25%, CO is about 4%, and CO<sub>2</sub> is about 17%.

From Table 8, we can see that the production of H<sub>2</sub> and CH<sub>4</sub> starts at a relatively lower temperature. The concentration of H<sub>2</sub> is 27%, CH<sub>4</sub> is 43%, CO is 12%, and CO<sub>2</sub> is 15% at 600 °C. At higher temperatures, like at 700 °C, the concentration of hydrogen increases significantly, the concentration of methane, carbon monoxide, and carbon dioxide decreases. At higher temperatures, the attention of evolving gas is almost the same as at 700 °C. The final gas composition produced during the pyrolysis of wheat straw is H<sub>2</sub> 50%, CH<sub>4</sub> is about 20%, CO is about 10% and 19% CO<sub>2</sub>.

Table 9 shows that the concentration of H<sub>2</sub> and CH<sub>4</sub> at 600 °C is significant, and CO, CO<sub>2</sub> are relatively low. H<sub>2</sub> concentration increases from 29 to 67% at elevated temperatures, but methane is almost the same at a higher temperature to about 25%. The concentration of CO and CO<sub>2</sub> is decreasing. The overall composition of H<sub>2</sub> is 49%, CH<sub>4</sub> is 20%, CO is 9%, and CO<sub>2</sub> is 20%.

From Table 10, we can see that hydrogen content is 34.6%, methane is 8.10%, carbon monoxide is very less than 1.33%, and CO<sub>2</sub> is 55% which is high in concentration at 600 °C. At higher temperatures yielding of hydrogen and methane is increasing, but carbon dioxide decreases. The overall volumetric concentration of the gaseous sample is H<sub>2</sub> 38%, methane 8%, carbon monoxide 1.62%, and very high carbon dioxide 51.8%.

## Mass and energy balance

Wt% of Biochar:  $W_1$  (Measured)

Wt% of Bio-oil:  $W_2$  (Measured)

Wt% of gas :  $W_3 = (100 - W_1 - W_2)$  (3)

CV<sub>o</sub>: calorific value and CV<sub>G</sub>: Calorific value in kcal/kg.

## Mass balance of gaseous product

Wt. of gas = (Volume of gas/22.4) \* Molecular weight of the gas.

From Tables 5, 6, 7, 8, 9 and 10, the mass balance is calculated.

## Energy balance

$$E_B = CV_B * M_B \quad (4)$$

$$E_C = CV_C * M_C \quad (5)$$

$$E_G = CV_G * M_G \quad (6)$$

$$E_O = CV_O * M_O \quad (7)$$

For CV<sub>B</sub>, CV<sub>C</sub> refer Table 2, and CV<sub>G</sub>, CV<sub>O</sub>,  $M_B$ ,  $M_C$ ,  $M_G$ ,  $M_O$  refer Table 11, whereas  $E_B$ —Energy of biomass; CV<sub>B</sub>—Calorific value of biomass (Kcal/kg);  $M_B$ —Weight of biomass;  $E_C$ —Energy of Char; CV<sub>C</sub>—Calorific value of char (Kcal/kg);  $M_C$ —Weight of Char;  $E_G$ —Energy of product gas; CV<sub>G</sub>—Calorific value of product gas (Kcal/kg);  $M_G$ —Mass of product gas;  $E_O$ —Energy of Bio-oil; CV<sub>O</sub>—Calorific value of Bio-oil (Kcal/kg),  $M_O$ : Weight of Bio-oil (Table 11).

Nearly 43, 30, 29, 24, 22, and 10% of the total energy of SH, PP, MS, WS, DH, and VT, respectively, in the process converts as gaseous energy and char, and oil remains in the sub-products (Table 12). Maximum hydrogen percent is in SH 9% and lowest in VT 3% by wt, and methane yield is maximum in PP 29% but lowest in VT 5% by wt; VT has

**Table 11** Mass balance of feed and product (wt%) CV of gas and oil

Sample name	Biomass	$W_1$	$W_2$	$W_3$	CV <sub>o</sub>	CV <sub>G</sub>
SH	100	31.11	39.95	28.94	844	6240
PP	100	36.15	38.23	25.62	2160	5322
MS	100	38.59	37.27	24.14	1860	5881
WS	100	37.64	40.78	21.58	2474	4755
DH	100	37.95	40.85	21.20	1578	4346
VT	100	33.44	45.47	21.09	3478	1549



**Table 12** Energy balance of feed and product in kcal/kg

Sample name	Biomass (kcal)	Char (kcal)	Bio-oil (kcal)	Product gas (kcal.)
SH	4143	1993	338	1812
PP	4454	2255	820	1379
MS	4264	2337	688	1239
WS	4081	2073	1014	994
DH	4184	2621	647	916
VT	3941	2007	1565	369

**Table 13** Estimated wt of different gaseous products

Sample name	H <sub>2</sub> (%)	CH <sub>4</sub> (%)	CO (%)	CO <sub>2</sub> (%)
SH	9.01	25.31	22.62	43.06
PP	7.22	21.84	22.91	48.03
MS	7.47	29.22	8.83	54.48
WS	6.40	20.27	17.79	55.54
DH	6.32	20.81	16.12	56.75
VT	3.00	5.38	1.79	89.83

highest carbon dioxide (Table 13). Maximum gaseous yield wt% is 29 in SH and VT has the lowest 21% gas yields but maximum oil 45% in VT (Table 11).

The conversion system has some energy losses, such as endothermic and exothermic reactions, which happen during the process. These losses are not considered in the calculation of mass and energy balance. However, according to Jesus et al. (2018), these losses are unavoidable during the thermal decomposition of biomass.

Below 600 °C temperatures, H<sub>2</sub> evolves in a lesser amount, and lignin becomes the main compound responsible for the formation of H<sub>2</sub> (Amutio et al. 2012). The groups present in the hemicelluloses (C=O, C–O, C–C) and the linear polymer chain of cellulose are responsible for CO and CO<sub>2</sub>. The secondary chemical reactions like decarboxylation and depolymerization of volatile materials during pyrolysis also produce CO<sub>2</sub> (Yang et al. 2007; Jesus et al. 2018).

### Application of BIO-HCNG in a 2KVA petrol genset for power production

As shown in Fig. 3, the flame is very light blue, indicating that the gaseous mixture is rich in hydrogen and methane, which is highly suitable for the internal combustion engines for the transportation sector (H<sub>2</sub>Property).

**Fig. 3** Flame of hydrogen- and methane-rich produced gas from the stepped pyrolysis of biomass

The existing IC engine, without any significant modification, can be run on H-CNG. The existing CNG dispensing refueling infrastructure can deliver H-CNG blends with minimal upgradation (Pradhan and Kailashgahlot 2020). This study uses pyrolytic gas (High hydrogen content in CNG) as fuel in petrol Genset. However, the Genset is functioning smoothly without any extra noise and hindrance. Furthermore, fuel cleaning requires for the long run of Genset or smooth performance. The work focuses on utilizing the bio-waste to generate high hydrogen-containing fuel, applicable to IC engines. Hydrogen-enriched methane as a fuel for SI engines shows a significant economic and positive impact on efficiency (Nanthagopal et al. 2011).

In this study, the high hydrogen content CNG product gas is utilized directly to petrol Genset engine, further particulate matters and tarry particles removed by (rice husk and cotton adsorption techniques) scrubber. However, hydrogen separation from the pyrolytic gas can be through pressure swing adsorption (PSA) (Grande 2012; Siew et al. 2013) or cryogenic separation technique, which needs to be further studied (Chang et al. 2008).

A 2KVA Honda petrol Genset was modified for gaseous fuel to utilize the available hydrogen-rich mixture of gaseous fuel from the process. Genset was functioning from the non-condensable gases of the pyrolysis process. As the

mixture was hydrogen-rich, the Genset creates lesser sound and shows smooth functioning than gasoline fuel. The generator was subjected to full load (1 exhaust of 1KVA, one cooler of 0.2KVA, one pump of 0.7KVA).

Table 14 shows the duration of Genset, electricity produced using different biomass samples as input (2.5 kg biomass) to the reactor and using hydrogen-rich mixture gas as fuel to the Genset.

**Economy analysis**

- Fuel consumption (Biomass): 2.5 kg/run.
- Labor cost: 500 Rs /day.
- Electricity cost in India: 6 Rs/unit.
- Price of petrol in India: 100 Rs/l.
- Reactor power rating: 4 kWh.
- Cost of operation of the equipment: 20 Rs. (50 min run, consume 3.3 kW energy).
- Overhead cost: 3 Rs./kg of raw biomass.
- Cost of biochar: 18Rs./kg.
- Cost of crude bio-oil: 5 Rs./kg.
- Fuel consumption (Petrol): 500 ml/h.

$$\text{Total cost } (C_{BI})(Rs.) = \text{Feed cost} + \text{Processing cost} + \text{Overhead cost} \tag{8}$$

$$\begin{aligned} \text{Output cost after processing } (C_{BO})(Rs.) &= \text{Cost of biochar} * \text{weight of char} \\ &+ \text{Cost of Bio - oil} * \text{weight of bio - oil} + \text{cost of electricity produced from Genset from gas} \end{aligned} \tag{9}$$

$$\text{Total cost of Petrol } (C_{PI})(Rs.) = \text{Petrol consumption } (L) * \text{Unit cost of petrol} \tag{10}$$

$$\text{Output cost from Genset } (C_{PO})(Rs.) = \text{Unit price of electricity} * \text{total unit of electricity produced} \tag{11}$$

$$E_1 = (C_{BO}/C_{BI}) * 100 (\%) \tag{12}$$

$$E_2 = (C_{PO}/C_{PI}) * 100 (\%) \tag{13}$$

For feed cost; weight of char and oil; run duration and efficiency refer to Tables 1, 11, 14, and 15 respectively.

**Mathematical analysis**

Mathematical analysis was done to obtain correlations MODEL-1, between running time of Genset (refer Table 14) to net hydrogen (refer raw to char composition, wt% from Table 3) as well as the cumulative volumetric percentage of hydrogen and methane (refer to Tables 5, 6, 7, 8, 9, and 10, overall rows). And MODEL-2 between running time of Genset (refers to Table 14) to net hydrogen (refer raw to char composition, wt% from Table 3) as well as hydrogen percent, and methane percent of product gas separately (refer Tables 5, 6, 7, 8, 9, and 10, overall rows). The derived model is shown in Table 16.

Data from Tables 3, 5, 6, 7, 8, 9, 10 and 14 are used to develop a correlation for estimating the running duration of the 2KVA Genset. The correlation is developed using

**Table 14** Running duration of Genset (in minutes) using produced H<sub>2</sub>-rich mixture of gases from different biomass samples

Sample Name	SH	PP	MS	WS	DH	VT
Duration (minute)	30	27	28	26	26	16

**Table 15** Efficiency table

Sample name	Biomass			Petrol			E <sub>1</sub> /E <sub>2</sub>
	C <sub>BI</sub>	C <sub>BO</sub>	E <sub>1</sub>	C <sub>PI</sub>	C <sub>PO</sub>	E <sub>2</sub>	
SH	33.75	25.00	74.07	25	6	24.00	3.08
PP	32.50	26.40	81.23	22.50	5.4	24.00	3.38
MS	32.50	27.53	84.70	23.33	5.6	24.00	3.53
WS	35.00	27.22	77.77	21.67	5.2	24.00	3.24
DH	31.25	27.40	87.68	21.67	5.2	24.00	3.65
VT	31.25	24.02	76.86	13.33	3.2	24.00	3.20

**Table 16** Derived MODEL-1 and MODEL-2 based on different parameters ( $\Delta H$ , CG,  $H_2$ , and  $CH_4$ )

Source	MODEL-1			MODEL-2		
	<i>p</i> Value ( $10^{-2}$ )	VIF	Regression Eq	<i>p</i> Value ( $10^{-2}$ )	VIF	Regression Eq
Regression	0.2	–	$D = -6.25 + 0.99\Delta H + 0.39CG$	0.4	–	$D = -9.20 + 0.09\Delta H + 0.61H_2 + 0.19CH_4$
$\Delta H$	18.6	1.32		85.1	2.62	
CG	0.1	1.32		–	–	
$H_2$	–	–		1.5	7.72	
$CH_4$	–	–		10.7	4.92	

$D$  = Running duration of Genset;  $\Delta H$  = Change in hydrogen wt% during the pyrolysis process; CG = Cumulative volumetric gas % of ( $H_2$  &  $CH_4$ ) obtained from gas chromatography;  $H_2$  = Volumetric gas % of hydrogen reported in gas chromatography;  $CH_4$  = Volumetric gas % of methane reported in gas chromatography

the least square regression analysis in MINITAB 19.2020 software.

### Model summary

From the regression analysis,  $R$ -square value = 0.98 for model-1 and  $R$ -square = 0.99 for Model-2. As the value of  $R$ -square is greater than 0.95, it shows a good correlation between dependent and independent variables (Gautam 2017).

### Analysis of variance

The value of  $P$  indicates the effect of the independent variable on the dependent variable; the lower the  $p$  value higher the impact on the dependent variable. Table 11, in model-1, the  $p$  value for both independent variables is very close to zero, which implies that  $\Delta H$  and CG contribute significantly. In model-2, the  $p$  value of  $\Delta H$  is higher than  $H_2$  and  $CH_4$ , so  $\Delta H$  is less significant than  $H_2$  and  $CH_4$ .

The desired value of VIF (variance inflation factor) should be closer to 1. A higher value indicates undesirable multicollinearity. In model-1, the VIF value is 1.32 for both independent variables, whereas, in model-2, the VIF values are 2.62, 7.72, and 4.92 for different independent variables.

From the above analysis of variance, the effect of the independent variable in model-1 is more significant than model-2. So the consideration of parameters  $\Delta H$ , CG is more appropriate than  $\Delta H$ ,  $H_2$ , and  $CH_4$  for estimating the running time of Genset.

### Residual plots for duration

From Fig. 4a, the data are very close to the fitted line, and the line represents the regression equation. From Fig. 4b, the histogram shows the normally distributed data, which means the regression equation holds the value beyond the

table; in Fig. 4a', the data have relatively more deviation from the fitted line, and Fig. 4b' shows that the data are not distributed normally.

### Conclusion

The biomass like sun hemp, pigeon pea, mustard stem, wheat straw, vantulasi, and dhaincha is categorized as high hydrogen content crops. It resulted in hydrogen-rich product gas during stepped pyrolysis. Hydrogen and methane production was directly proportional to temperature; however, higher temperature ranges contributed more to hydrogen and methane production. Depending on different biomass samples, non-condensable biogases typically contained 40–55 vol% hydrogen, 8–25 vol% methane, 1–12 vol% carbon monoxide, and 12–50 vol% carbon dioxide. The concentration of hydrogen increases with an increase in temperature; however, the methane concentration decreases except mustard stem and vantulasi. The CO and  $CO_2$  gas concentrations decrease with an increase in temperature except for vantulasi, in which CO concentration increases. Product gas composition shows sun hemp having the highest (57.22% by vol.) hydrogen and mustard stem having the highest (25.65% by vol.) methane among all biomass samples. High hydrogen and methane-containing pyrolytic fuel are efficient for IC engines. Among all the samples, the performance of pyrolytic gas in 2KVA Honda petrol Genset is highest 12 min/kg in Sun hemp and lowest 6.4 min/kg in Vantulasi. The electricity production from Genset is very efficient with obtained product gas than petrol. However, the highest process efficiency is 87% for dhaincha and 74% for sun hemp, which is 3.6 times and 3 times respectively more effective than petrol in Genset for power production. A mathematical correlation between net hydrogen ( $\Delta H$ ), hydrogen gas ( $H_2$ ), and methane gas ( $CH_4$ ) is developed and found that the MODEL-1 ( $D = -6.25 + 0.99\Delta H + 0.39CG$ )

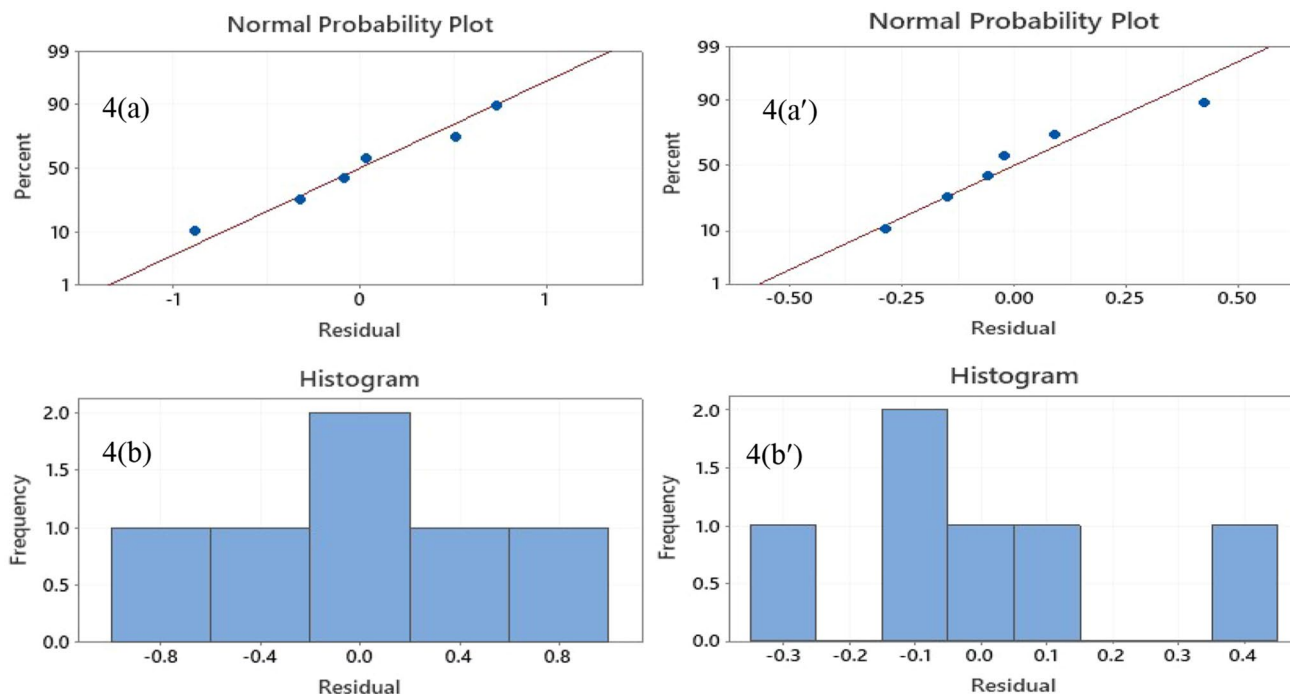


**Fig. 4** Normal probability plot and histogram for MODEL-1, denoted by (a, b) and for MODEL-2 denoted by (a', b')

is well-fitted over MODEL-2 ( $D = -9.20 + 0.09\Delta H + 0.61 H_2 + 0.19CH_4$ ).


**Acknowledgements** Author Brijesh Kumar Prajapati is thankful to the Department of Fuel Minerals and Metallurgical Engineering, Indian Institute of Technology (ISM) DHANBAD, and Department of Ceramic Engineering IIT (BHU) for carrying out this research work. This research did not receive any specific grant from funding agencies in the public, commercial, or not-for-profit sectors.

## References

- Abuadala A, Dincer I (2012) A review on biomass-based hydrogen production and potential applications. *Int J Energy Res* 36:415–455. <https://doi.org/10.1002/er.1939>
- Amutio M, Lopez G, Artetxe M et al (2012) Influence of temperature on biomass pyrolysis in a conical spouted bed reactor. *Resour Conserv Recycl* 59:23–31. <https://doi.org/10.1016/j.resconrec.2011.04.002>
- Balat M, Kirtay E (2010) Major technical barriers to a “hydrogen economy.” *Energy Sources Part A Recovery Util Environ Eff* 32:863–876. <https://doi.org/10.1080/15567030802606293>
- Chang K, Li Q, Li Q (2008) Refrigeration cycle for cryogenic separation of hydrogen from coke oven gas. *Front Energy Power Eng China* 2:484–488. <https://doi.org/10.1007/s11708-008-0096-0>
- Chang ACC, Chang HF, Lin FJ et al (2011) Biomass gasification for hydrogen production. *Int J Hydrog Energy* 36:14252–14260
- Chen G, Andries J, Luo Z, Spliethoff H (2003) Biomass pyrolysis/gasification for product gas production: the overall investigation of parametric effects. *Energy Convers Management* 44:1875–1884
- Chimpae S, Wongsakulphasatch S, Vivanpatarakij S, Glinrun T, Wiwatwongwana F, Maneeparakorn W, Assabumrungrat S (2019) Syngas production from combined steam gasification of biochar and a sorption-enhanced water-gas shift reaction with the utilization of CO<sub>2</sub>. *Processes* 7:349
- David B, Federico B, Cristina C et al (2019) Biohythane production from food wastes. In: Pandey A, Venkata Mohan S, Chang J-S, Hallenbeck PC, Larroch C (eds) *Biohydrogen*. Elsevier, Amsterdam, pp 347–368
- Debdoubi A, El Amarti A, Colacio E et al (2006) The effect of heating rate on yields and compositions of oil products from esparto pyrolysis. *Int J Energy Res* 30:1243–1250. <https://doi.org/10.1002/er.1215>
- Domínguez A, Menéndez JA, Fernández Y et al (2007) Conventional and microwave induced pyrolysis of coffee hulls for the production of a hydrogen rich fuel gas. *J Anal Appl Pyrolysis* 79:128–135. <https://doi.org/10.1016/j.jaap.2006.08.003>
- Dufour A, Girods P, Masson E et al (2009) Synthesis gas production by biomass pyrolysis: effect of reactor temperature on product distribution. *Int J Hydrog Energy* 34:1726–1734. <https://doi.org/10.1016/j.ijhydene.2008.11.075>
- Edwards P, Kuznetsov V, David WI (2007) Hydrogen energy. *Philos Trans R Soc A Math Phys Eng Sci* 365:1043–1056. <https://doi.org/10.1098/rsta.2006.1965>
- Enweremadu CC, Ojediran JO (2004) Evaluation of energy potential in husks from SOY-BEAN and COWPEA
- Gautam S (2017) Effect of washing and stamping on coke making of a low-grade Indian coal: correlation between various properties. *Ironmak Steelmak* 44:505–512. <https://doi.org/10.1080/03019233.2016.1217115>
- Grande CA (2012) Advances in pressure swing adsorption for gas separation. *Int Sch Res Not* 2012:100–102. <https://doi.org/10.5402/2012/982934>
- Green-talk Did you know there are 4 type of Tulsi in India? | Nurserylive. <https://nurserylive.com/blogs/plant-talk/did-you-know-there-are-4-type-of-tulsi-in-india>. Accessed 4 Aug 2021

- Gunaseelan VN (1997) Anaerobic digestion of biomass for methane production: a review. *Biomass Bioenergy* 13:83–114. [https://doi.org/10.1016/S0961-9534\(97\)00020-2](https://doi.org/10.1016/S0961-9534(97)00020-2)
- H<sub>2</sub>Property basic hydrogen propertylh2 tool. <https://h2tools.org/hyarc/hydrogen-data/basic-hydrogen-properties>. Accessed 15 Oct 2020
- Hernandez-Mena LE, Pecora AAB, Beraldo AL (2014) Slow pyrolysis of bamboo biomass: analysis of biochar properties. *Chem Eng Trans* 37:115–120. <https://doi.org/10.3303/CET1437020>
- Hlavsová A, Corsaro A, Raclavská H et al (2014) Syngas production from pyrolysis of nine composts obtained from nonhybrid and hybrid perennial grasses. *Sci World J*. <https://doi.org/10.1155/2014/723092>
- IISCRReport state-wise biomass data based on survey data of year [2002–04] for season : Agro-Kharif. Biomass resource atlas of India. Accessed 4 Aug 2021
- Jesus MS, Napoli A, Trugilho PF et al (2018) Energy and mass balance in the pyrolysis process of eucalyptus wood. *Cerne* 24:288–294. <https://doi.org/10.1590/01047760201824032561>
- Jiang H, Wu Y, Fan H, Ji J (2012) Hydrogen production from biomass pyrolysis in molten alkali. *AASRI Procedia* 3:217–223. <https://doi.org/10.1016/j.aasri.2012.11.036>
- Karagöz S (2009) Energy production from the pyrolysis of waste biomasses. *Int J Energy Res* 33:576–581. <https://doi.org/10.1002/er.1493>
- Lang Y, Arnepalli RR, Tiwari A (2011) A review on hydrogen production: methods, materials and nanotechnology. *J Nanosci Nanotechnol* 11:3719–3739
- Li S, Xu S, Liu S et al (2004) Fast pyrolysis of biomass in free-fall reactor for hydrogen-rich gas. *Fuel Process Technol* 85:1201–1211
- Liu Z, Si B, Li J et al (2018) Bioprocess engineering for biohythane production from low-grade waste biomass: technical challenges towards scale up. *Curr Opin Biotechnol* 50:25–31
- Liu P, Wang Y, Zhou Z et al (2020) Effect of carbon structure on hydrogen release derived from different biomass pyrolysis. *Fuel*. <https://doi.org/10.1016/j.fuel.2020.117638>
- Loison R, Foch P, Boyer A (1989) *Coke quality and production*. Butterworth & CO., London
- Luo G, Xie L, Zhou Q, Angelidaki I (2011) Enhancement of bioenergy production from organic wastes by two-stage anaerobic hydrogen and methane production process. *Bioresour Technol* 102:8700–8706. <https://doi.org/10.1016/j.biortech.2011.02.012>
- Luque R, Campelo J, Clark J (2011) *Handbook of biofuels production: Processes and technologies*. Woodhead Publishing, Sawston
- Mazzotti M, Carlos J, Allam R et al (2005) Mineral carbonation and industrial uses of carbon dioxide. In: IPCC special report on carbon dioxide capture and storage. pp 319–338
- Mengjie W, Suzhen D (1994) A potential renewable energy resource development and utilization of biomass energy. AGRIS Mnrereport Current Status | Ministry of New and Renewable Energy, Government of India. <https://mnre.gov.in/bio-energy/current-status>. Accessed 4 Aug 2021
- Momin SA, Dutta M, Kader G, Iftakher S (2016) Study of LPG (liquefied petroleum gas) and CNG (compressed natural gas) vehicles and its future aspects
- Moreno F, Muñoz M, Arroyo J et al (2012) Efficiency and emissions in a vehicle spark ignition engine fueled with hydrogen and methane blends. *Int J Hydrog Energy* 37:11495–11503. <https://doi.org/10.1016/j.ijhydene.2012.04.012>
- Mu Y, Wang G, Yu H-Q (2006) Kinetic modeling of batch hydrogen production process by mixed anaerobic cultures. *Bioresour Technol* 97:1302–1307. <https://doi.org/10.1016/j.biortech.2005.05.014>
- Nanthagopal K, Subbarao R, Elango T et al (2011) Hydrogen enriched compressed natural gas (HCNG)-a futuristic fuel for internal combustion engines. *Therm Sci* 15:1145–1154
- Neves D, Thunman H, Matos A et al (2011) Characterization and prediction of biomass pyrolysis products. *Prog Energy Combust Sci* 37:611–630
- Nunes LJR, Matias JCDO, Catalao JPDS (2017) *Torrefaction of biomass for energy applications: from fundamentals to industrial scale*. Academic Press, Cambridge
- Nunes LJR, De Oliveira Matias JC, Da Silva Catalão JP (2018) Introduction. In: Nunes LJR, De Oliveira Matias JC, Da Silva Catalão JP (eds) *Torrefaction of Biomass for Energy Applications*. Elsevier, Amsterdam, pp 1–43
- Paul A, Rahaman MA (2015) Potential of biomass based electricity generation in India: a case study. p 15
- Pawar SS, Nkemka VN, Zeidan AA et al (2013) Biohydrogen production from wheat straw hydrolysate using *Caldicellulosiruptor saccharolyticus* followed by biogas production in a two-step uncoupled process. *Int J Hydrog Energy* 38:9121–9130. <https://doi.org/10.1016/j.ijhydene.2013.05.075>
- Pradhan SD, Kailashgahlot S (2020) Providing clean and reliable energy supplies to meet the requirements is the top most priority of the Government, says Shri Dharmendra Pradhan Shri Pradhan inaugurates H-CNG Plant and Launches trials in Delhi
- Raveendran K, Ganesh A, Khilar KC (1996) Pyrolysis characteristics of biomass and biomass components. *Fuel* 75:987–998. [https://doi.org/10.1016/0016-2361\(96\)00030-0](https://doi.org/10.1016/0016-2361(96)00030-0)
- Reşitoğlu IA, Altinişik K, Keskin A (2015) The pollutant emissions from diesel-engine vehicles and exhaust aftertreatment systems. *Clean Technol Environ Policy* 17:15–27
- Ronsse F, van Hecke S, Dickinson D, Prins W (2013) Production and characterization of slow pyrolysis biochar: influence of feedstock type and pyrolysis conditions. *GCB Bioenergy* 5:104–115. <https://doi.org/10.1111/gcbb.12018>
- Sadhukhan J, Lloyd J, Scott K, Premier GC, Yu EH, Curtis T, Head IM (2016) A critical review of integration analysis of microbial electrosynthesis (MES) systems with waste biorefineries for the production of biofuel and chemical from reuse of CO<sub>2</sub>. *Renew Sustain Energy Rev* 56:116–132
- Siew K, Zhang N, Sadhukhan J (2013) Techno-economic analysis of poly-generation systems with carbon capture and storage and CO<sub>2</sub> reuse. *Chem Eng J* 219:96–108. <https://doi.org/10.1016/j.cej.2012.12.082>
- Suman S, Gautam S (2017) Pyrolysis of coconut husk biomass: analysis of its biochar properties. *Energy Sources Part A Recovery Util Environ Eff* 39:761–767. <https://doi.org/10.1080/15567036.2016.1263252>
- Suman S, Panwar DS, Gautam S (2017) Surface morphology properties of biochars obtained from different biomass waste. *Energy Sources Part A Recovery Util Environ Eff* 39:1007–1012. <https://doi.org/10.1080/15567036.2017.1283553>
- Xu Q, Lan P, Zhang B et al (2010) Hydrogen production via catalytic steam reforming of fast pyrolysis bio-oil in a fluidized-bed reactor. *Energy Fuels* 24:6456–6462. <https://doi.org/10.1021/ef1010995>
- Yang H, Yan R, Chen H et al (2007) Characteristics of hemicellulose, cellulose and lignin pyrolysis. *Fuel* 86:1781–1788. <https://doi.org/10.1016/j.fuel.2006.12.013>
- Zareei J, Haseeb M, Ghadamkheir K, Farkhondeh SA (2020) Science-Direct the effect of hydrogen addition to compressed natural gas on performance and emissions of a DI diesel engine by a numerical study. *Int J Hydrog Energy*. <https://doi.org/10.1016/j.ijhydene.2020.09.027>
- Zhao Z, Huang H, Wu C et al (2001) Biomass pyrolysis in an argon/hydrogen plasma reactor. *Eng Life Sci* 1:197. [https://doi.org/10.1002/1618-2863\(200111\)1:5%3c197::aid-elsc197%3e3.0.co;2-8](https://doi.org/10.1002/1618-2863(200111)1:5%3c197::aid-elsc197%3e3.0.co;2-8)

## Authors and Affiliations

Brijesh Kumar Prajapati<sup>1</sup> · Amrit Anand<sup>1</sup> · Shalini Gautam<sup>1</sup>  · Preetam Singh<sup>2</sup>

<sup>1</sup> Department of Fuel Minerals and Metallurgical Engineering,  
IIT(ISM), Dhanbad, Jharkhand 826004, India

<sup>2</sup> Department of Ceramic Engineering, IIT BHU, Varanasi,  
Uttar Pradesh 221005, India